



## LJMU Research Online

**Davies, MJ, Leach, AG, Fullwood, DL, Mistry, D and Hope, A**

**The pH Dependent Interaction between Nicotine and Simulated Pulmonary Surfactant Monolayers with Associated Molecular Modelling**

<http://researchonline.ljmu.ac.uk/6281/>

### Article

**Citation** (please note it is advisable to refer to the publisher's version if you intend to cite from this work)

**Davies, MJ, Leach, AG, Fullwood, DL, Mistry, D and Hope, A (2017) The pH Dependent Interaction between Nicotine and Simulated Pulmonary Surfactant Monolayers with Associated Molecular Modelling. Surface and Interface Analysis. ISSN 1096-9918**

LJMU has developed **LJMU Research Online** for users to access the research output of the University more effectively. Copyright © and Moral Rights for the papers on this site are retained by the individual authors and/or other copyright owners. Users may download and/or print one copy of any article(s) in LJMU Research Online to facilitate their private study or for non-commercial research. You may not engage in further distribution of the material or use it for any profit-making activities or any commercial gain.

The version presented here may differ from the published version or from the version of the record. Please see the repository URL above for details on accessing the published version and note that access may require a subscription.

For more information please contact [researchonline@ljmu.ac.uk](mailto:researchonline@ljmu.ac.uk)

<http://researchonline.ljmu.ac.uk/>

# The pH Dependent Interaction between Nicotine and Simulated Pulmonary Surfactant Monolayers with Associated Molecular Modelling

Michael J. Davies<sup>a,\*</sup>, Andrew G. Leach<sup>a</sup>, Danielle Fullwood<sup>a</sup>, Dinesh Mistry<sup>a</sup> & Alexandra Hope<sup>a</sup>

<sup>a</sup>The School of Pharmacy and Biomolecular Sciences, Liverpool John Moores University, Liverpool, L3 3AF, UK.

## Abstract

Pulmonary surfactant is an endogenous material that lines and stabilises the alveolar air-liquid interface. Respiratory mechanics can be compromised by exposure to environmental toxins such as cigarette vapour, which contains nicotine. This study aims to determine the influence of nicotine on the activity of simulated lung surfactant at pH 7 and pH 9. In all cases, the addition of nicotine to the test zone caused deviation in surfactant film performance. Importantly, the maximum surface pressure was reduced for each system. Computational modelling was applied to assess key interactions between each species, with the Gaussian 09 software platform used to calculate electrostatic potential surfaces. Modelling data confirmed either nicotine penetration into the two-dimensional structure or interfacial / electrostatic interactions across the underside. The results obtained from this study suggest that nicotine can impair the ability of pulmonary surfactant to reduce the surface tension term, which can increase the work of breathing. When extrapolated to gross lung function alveolar collapse and respiratory disease (e.g. chronic airway obstruction) may result. The delivery of nicotine to the (deep) lung can cause a deterioration in lung function and lead to reduced quality of life.

## Key words

Pulmonary surfactant, Langmuir monolayers, nicotine, cigarette vapour, molecular modelling, Gaussian 09.

## Corresponding Author Details:

\* To whom correspondence should be addressed:

Tel. (+44) 0151 231 2024

Email: [m.davies1@ljmu.ac.uk](mailto:m.davies1@ljmu.ac.uk)

Fax. (+44) 0151 231 2170

## 1. Introduction

Pulmonary surfactant plays a critical role in the respiratory system. This endogenous material preserves airway patency by adsorbing at the alveolar air-liquid interface and reducing the surface tension term to near zero values. The substance is a complex, multicomponent mixture containing phospholipids along with specific protein molecules (i.e. SP-A, SP-B, SP-C and SP-D), which is secreted by type II epithelial cells located in the alveolar space [1]. Phospholipid molecules account for approximately 90% of the blend by weight and of these dipalmitoylphosphatidylcholine (DPPC) predominates [2]. Additional species include saturated and unsaturated phosphatidylglycerols (e.g. POPG), unsaturated phosphatidylcholine and anionic lipids. Molecules such as cholesterol, triglycerides and fatty acids form the remainder of the material [3]. As a result of the inherent arrangement at the alveolar air-liquid interface, pulmonary surfactant is the point of first contact for any material inhaled from the external environment.

DPPC is responsible for reducing the surface tension term to near zero values in the alveolar space. At 41°C DPPC displays a gel to liquid phase transition and as such the molecule exists in an ordered state at body temperature [4 & 5]. Here, there is capacity for the saturated fatty acyl chains to pack together closely with supportive electrostatic interactions between oppositely charged portions of the polar head groups [6]. As a result DPPC adsorbs very slowly at the air-liquid interface [5], which limits overall spreadability. Thus, for the surfactant film to function effectively, additional species such as phosphatidylglycerols, cholesterol, unsaturated phospholipids and proteins are naturally incorporated within the blend. The DPPC molecule is zwitterionic in nature and composed of two saturated, 16-carbon palmitic chains that are attached to a negatively charged phosphate group and ultimately a positively charged trimethylammonium moiety [7]; the molecular structure of the species is detailed in Figure 1a. In addition to charge-charge interactions, the inherent chemistry enables the molecule to serve as both a C-H hydrogen bond donor (i.e. via the trimethylammonium group) and a hydrogen bond acceptor (via the phosphate oxygen atoms) [8]. Furthermore, both the charged phosphate and trimethylammonium groups may also have the capability of forming ionic bonds with suitably charged species in solution.

The POPG molecule is of anionic character and exhibits chemistries similar to DPPC [9]. This molecule increases the fluidity of the surfactant monolayer at the alveolar air-liquid interface and thereby enhances the respreading profile on inhalation [9]. This effect is achieved by increasing the two-dimensional ordering of the DPPC molecules plus the inherent molecular flexibility [10]. Furthermore, both the attractive and repulsive intermolecular electrostatic forces and hydrogen bonding between zwitterionic DPPC and anionic POPG polar head groups supports optimal packing behaviour and thus surfactant function [6]. The key differences in chemical arrangement when compared to DPPC involve an unsaturated fatty acid chain attached to the charged phosphate group and the presence of a hydrocarbon chain attached to two hydroxyl groups in place of the trimethylammonium functionality [11]. The resulting chemistries enable POPG to function as either a hydrogen bond acceptor or donor when interacting with molecules dissolved in the supporting aqueous subphase [8]. In addition, each hydroxyl group holds the potential to form intermolecular bonds between neighbouring molecules or intramolecular bonds within one molecule [12].

Palmitic acid is 16-membered, saturated fatty acid with a terminal carboxylic acid group; the molecular arrangement is presented in Figure 1c [1, 10 & 13]. This molecule is frequently included within commercially available surfactant replacement preparations (e.g. Survanta) to facilitate material respreading at the alveolar air-liquid interface [2]. Furthermore, the incorporation of palmitic acid into a surfactant monolayer increases viscosity and the strength of solid domains rich in DPPC [2, 13 & 14]. The ionised carboxylic acid functionality inherent within the molecule may serve as a hydrogen bond acceptor within aqueous media. As such, the moiety is able to experience lateral electrostatic interactions and form charge-enhanced hydrogen bonds with the polar head groups of DPPC and POPG [15].

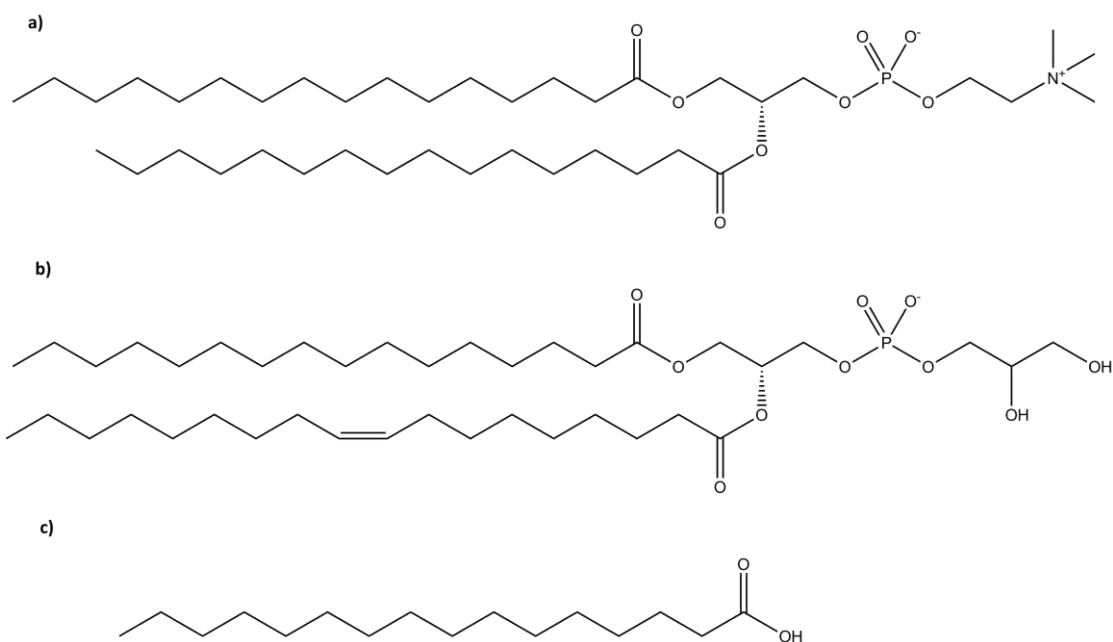


**Figure 1.** The molecular structures of (a) DPPC, (b) POPG and (c) PA.

Langmuir monolayers composed of phospholipid molecules and surfactant-specific proteins may be applied within the research setting as models to mimic the alveolar air-liquid interface [16]. In an identical fashion to the lung, the amphiphilic molecules arrange themselves such that the fatty acyl chains are displaced away from the aqueous subphase while the polar head groups make direct contact [3]. Lateral forces may be applied to the monomolecular films in isolation or indeed quick succession to obtain expansion / compression cycles reflective of typical human breathing patterns [17]. Langmuir pressure-area ( $\pi$ -A) isotherms may be applied to demonstrate the structure-function activity profile of amphiphilic material in response to challenge with active pharmaceutical ingredients or environmental toxins (i.e. nicotine).

Tobacco vapour is composed of over 4000 compounds, containing toxic chemicals, irritants and over 60 carcinogens [18]. It is estimated that the use of tobacco causes approximately 6 million deaths worldwide per annum and it is thus regarded as a significant public health concern [19]. Tobacco smoke may be classified as either mainstream smoke (i.e. that inhaled by the smoker) or environmental tobacco smoke (ETS) (i.e. the smoke emitted from a lit cigarette plus exhaled mainstream smoke). As previously alluded to, upon inhalation of tobacco smoke pulmonary surfactant is the first point of contact for the range of compounds held within the aerosolised vapour [3].

Thus, the interaction between the major components (e.g. nicotine) and the molecular species forming the surfactant material is an important influence on gross lung function. To this end, in 2003 Bringezu and co-workers reported that after exposure to ETS surfactant, efficacy and stability was reduced. Here, alterations in lipid composition and distribution were thought to influence surfactant respreading thus causing inadequate coverage at the air-liquid interface on expansion. The group proposed that impairments in pulmonary surfactant structure-function activity can compromise lung function [1].

Nicotine is a naturally occurring alkaloid that is both highly addictive and toxic [20]. The substance is one of many emitted from cigarettes upon use and accounts for approximately 0.5 - 2.0 mg by mass of each unit. Typically, a total of 20% of nicotine inhaled by the consumer is rapidly absorbed into the bloodstream [21]. The net effect is the increase in central dopamine and noradrenaline levels that evoke an instant change in mood (i.e. provide feelings of pleasure, reduced stress and anxiety). The nicotine molecule (3-(1-methyl-2-pyrrolidiniyl)-pyridine) is considered to be a weak organic base owing to the presence of two nitrogen atoms that function as proton-acceptor sites [22]. The species is composed of a 5-membered pyrrolidine ring of pKa 8.02 that contains its nitrogen atom in the more basic sp<sup>3</sup> configuration and a 6-membered pyridine ring of pKa 3.12 in which the nitrogen atom is in the sp<sup>2</sup> configuration [23]. Nicotine can exist as the cis- or trans- stereoisomer (with regards to the relative position of the pyridine and methyl groups) with interchange between the two being rapid; the molecular structure of the nicotine molecule is illustrated in Figure 2.



**Figure 2.** *The chemical structure of nicotine.*

Variation in the protonation state of this molecule is dependent on solution pH. For example, below pH 3 the diprotonated species exists, between pH 4-7 the monoprotonated form presents (due to the protonation of N-methyl-pyrrolidine) and above pH 9 nicotine exists as a neutral molecule [22]. Therefore at physiological pH, the predominant species are the singly protonated pyrrolidinium form and the neutral form [24]. Further to protonation of the nitrogen atoms, potential exists for the nicotine molecule to interact attractively with either the negatively charged functionalities within pulmonary surfactant (i.e. the negatively charged phosphate groups of DPPC and POPG) forming ionic bonds or indeed with the hydrogen bond donors (i.e. hydroxyl groups) resulting in ion-dipole interactions. Repulsive electrostatic interactions with the positively charged ammonium groups may be a necessary consequence of the proximity required to form these attractive interactions.

The surface electrostatic potentials for nicotine and the polar regions of DPPC, POPG and PA may be calculated via application of quantum mechanics, as exemplified by studies of halogen bonding and aromatic- $\pi$  anion interactions [25 & 26]. Such information can lend support to further understand important molecular interactions between each species and how key functionalities orientate themselves when in close contact. Density functional theory can provide electrostatics of sufficient accuracy to explain interactions [27]. This approach will be applied to rationalise information obtained from Langmuir monolayer studies such that deviations in the isotherms from the normal can be mechanistically explained.

This study aims to probe the response of simulated pulmonary surfactant monolayers to the application of nicotine within aqueous environments at pH 7 and pH 9. A molecular modelling approach will be applied to rationalise key trends within the data. The results obtained will be extrapolated to the human respiratory system with potential implications to lung function considered.

## **2. Materials and Methods**

### *2.1 Materials*

(-)-Nicotine of 98.5% purity was purchased as Pestanal<sup>®</sup> from Sigma-Aldrich, UK (BN: SZBD102XV). The surfactants DPPC (Avanti Polar Lipids, USA. BN: 160PC-315), POPG (Avanti Polar Lipids, USA. BN: 160-181PG-131) and PA (Sigma-Aldrich, UK. BN: 087K1877) were of analytical grade and used as supplied. Chloroform (CHCl<sub>3</sub>) of analytical grade ( $\geq 99.9\%$ , VWR Chemicals, UK. BN: 14B200510) was employed as the spreading solvent.

Ultrapure water (Purite, UK), demonstrating a resistivity of 18.MΩcm, was used both during cleaning procedures and as the aqueous subphase. In order to achieve pH adjustment, appropriate volumes of sodium hydroxide (Fisher Scientific, Loughborough. BN: 1557941) were added to the aqueous subphase.

## 2.2 Method

### 2.2.1 Langmuir Monolayers

Surfactant monolayers were produced using a Langmuir trough (Model 102M, Nima Technology, UK). Surfactant-free Kimtech tissues (Kimtech Science, Kimberley-Clark Professional, 75512, UK) were soaked in chloroform and used to clean all the glassware and contacting surfaces. Test runs that monitor surface pressure during barrier compression were performed to ensure cleanliness. Cleanliness was considered to have been achieved when the surface pressure was below  $0.4\text{mNm}^{-1}$  at complete barrier compression, in the absence of a surfactant monolayer.

A spreading solution composed of DPPC, POPG and PA in the ratio 69:20:11 was produced by dissolving the surfactant material in chloroform ( $1\text{ mg ml}^{-1}$ ). In total  $10\mu\text{l}$  of this solution was delivered to the surface of the pure water subphase by drop-wise addition using a Hamilton microsyringe and left for 10 minutes to facilitate chloroform evaporation and surfactant spreading. The trough barriers were programmed to move to the centre of the trough at a rate of  $25\text{ cm}^2\text{ min}^{-1}$ . Plots of surface pressure vs. area per molecule for the surfactant system at ambient temperature (e.g.  $20^\circ\text{C}$ ) were collected using a Wilhelmy plate at the centre of the compartment.

### 2.2.2 Nicotine Administration to Simulated Pulmonary Surfactant Monolayers

Initially, a total of  $10\mu\text{l}$  of the nicotine stock solution was taken and diluted to 10ml with ultrapure water to provide a  $1\text{mg/ml}$  aqueous solution. A volume of either  $100\mu\text{l}$  or  $200\mu\text{l}$  of the diluted nicotine solution was injected underneath the simulated pulmonary surfactant monolayer via a Hamilton microsyringe at full film expansion in order to monitor dose-response effects. Subsequently, a period of 10 minutes was given to allow for nicotine-monolayer interaction and corresponding Langmuir isotherms / isocycles were then obtained for each system under investigation.



### 2.2.3 Control over System pH

Consideration was afforded to the interaction between nicotine and simulated pulmonary surfactant monolayers at pH 7 and 9. The pH of the subphase was adjusted by use of sodium hydroxide. The pH 7 system was readily established via collection of water from the purification platform. To achieve a subphase at pH 9, a total of 6 $\mu$ l of 0.2M sodium hydroxide was added to 60ml ultrapure water via a Gilson pipette and the resulting solution thoroughly mixed. The pH of all aqueous solutions was monitored by a digital pH meter (HANNA Instruments, pH211 Microprocessor pH Meter). In all cases three replicates at each pH were undertaken to ensure consistency of results. Each experiment was conducted over a relatively short timescale (e.g. 10 minutes as a maximum). Consequently, there would have been limited opportunity for significant amounts of atmospheric CO<sub>2</sub> to dissolve across the 70cm<sup>2</sup> surface and into the supporting subphase. As such, environmental impact on system pH was minimal.

### 2.2.4 Langmuir Monolayer Analysis

#### 2.2.4.1 Compressibility

To enable the assessment of the competence of a surfactant to reduce the surface tension with minimal changes to surface area [28], the compressibility term was calculated. Lung surfactant should ideally have a low compressibility value, which translates *in vivo* to gas exchange taking place over a larger surface area [28 & 29]. The lower the compressibility term, the more rigid the surfactant film is (i.e. the material is of low elasticity), with the opposite being true [30 & 31]. The formula used to obtain compressibility values for each surfactant system is provided in Equation 1.

$$\text{Compressibility} = \frac{1}{A} \times \frac{1}{m}$$

**Equation 1.** Calculation of the compressibility of the monolayer.

Where A represents the relative surface area and m the slope of the isotherm. Here, 'm' was calculated using  $m = \frac{y_2 - y_1}{x_2 - x_1}$ , over the range of 30-10mN/m surface pressure, whereby 'y' and 'x' values characterise surface pressure and area values, respectively. The area values were converted from angstroms squared per molecule ( $\text{\AA}^2/\text{molecule}$ ) to percentage trough area for this calculation to be conducted [28].

#### 2.2.4.2 Limiting area-per-molecule

The limiting area ( $A_{\text{lim}}$ ), or the area in the most condensed region of the monolayer, represents the cross-sectional area of the molecule in the monolayer and was obtained by extrapolating the linear liquid expanded-liquid condensed slope of the  $\pi$ -A isotherm to  $\pi = 0$  [32 & 33]. This parameter offers an insight into the molecular state within the monolayer, more specifically revealing whether the molecules are more condensed or expanded [32 & 33]. A higher value signifies loose molecular arrangement within the monolayer over a larger area, and thus represents an expansion. Whereas, a lower value indicates that a lower area is available to lipid molecules, resulting in a tightly-packed, condensed monolayer [34].

#### 2.2.4.3 Lift-off area

Lift-off area represents the point at which the surface pressure of the compression isotherm starts to rise from the baseline, it was determined by extrapolating this point to the horizontal 'area' axis of the surface pressure-area isotherm [28]. Lift-off area characterizes the molecular interactions and packing within the monolayer, providing a second numerical figure capable of reinforcing the 'limiting area-per-molecule' outcome, to further evidence molecular expansion or compression. Here, again, larger values indicate a more expanded state, whereby molecules are occupying a larger space with reduced intermolecular interactions, and vice versa [30].

#### 2.2.4.4 Area under the curve and hysteresis of isotherms

To further determine the compressibility of the monolayer, the area under the curve (AUC) term was calculated via Equation 2, namely the 'Trapezoid Rule'.

$$(A1 - A2) \times \frac{(P1 + P2)}{2}$$

**Equation 2.** Calculation of the AUC term.

Where  $A$  represents relative Langmuir trough area values (i.e. taken directly from the x axis) and  $P$  is the corresponding surface pressure term (i.e. taken directly from the y axis) at the given area. This calculation was undertaken throughout the whole isotherm area of 82-25mN/m at 5mN/m intervals, these values were successively totalled to provide the final AUC. The hysteresis area, a parameter that has restricted use to cyclic isotherms, was formulated as the difference between the area under the curve of compression and expansion [28]. The hysteresis area represents the variance between the free energy of compression and free energy of expansion.

#### 2.2.4.5 Statistical Analysis

All compression isotherms were carried out at least three times to ensure reproducibility, and compression-expansion cycles were conducted as duplicates. The standard deviation was calculated to produce standard error bars of the mean, which was calculated via Equation 3.

$$SE_x = \frac{s}{\sqrt{n}}$$

**Equation 3.** Calculation of standard error of the mean.

Where  $s$  is the sample standard deviation and  $n$  is the size (number of observations) of the sample. Significant differences can be visualised using these standard error bars of the mean; when the error bars of different isotherms do not intersect, this provides clear evidence that there is no overlap of data and ultimately, that meaningfully different values are existent.

### 2.2.5 Molecular Modelling

To visualise and rationalise the interactions between nicotine and key components of the simulated pulmonary surfactant monolayer (i.e. DPPC, POPG and PA) the structures were studied at the RHF/6-31G\* level using the Gaussian09 suite of programs [35, 36, 37 & 38]. Conformations of the key elements for molecular recognition (excluding the long hydrocarbon chains) were generated using omega [39]. After geometry optimisation, the electron density was visualised in Gaussview [40]. The electrostatic potential is projected onto a surface of constant electron density using default values within the program. Representations of the projected electrostatic potential were generated from two opposing sides. The protocol led to the generation of a number of images that represent all of the entities that could potentially interact at the test interface.

## 3 Results and Discussion

During this study, stable mixed surfactant films comprising DPPC, POPG and PA were established to mimic the endogenous material located at the alveolar air-liquid interface within the (deep) lung. As such, on compression and expansion those interactions taking place across the two-dimensional plane were reflective of those associations taking place during normal lung function within the body [41].

### *3.1 Baseline: Langmuir Isotherms at pH 7 and 9*

Langmuir pressure-area isotherms of monolayers composed of DPPC, POPG and PA on an ultrapure water subphase at pH 7 or pH 9 are presented in Figure 3.

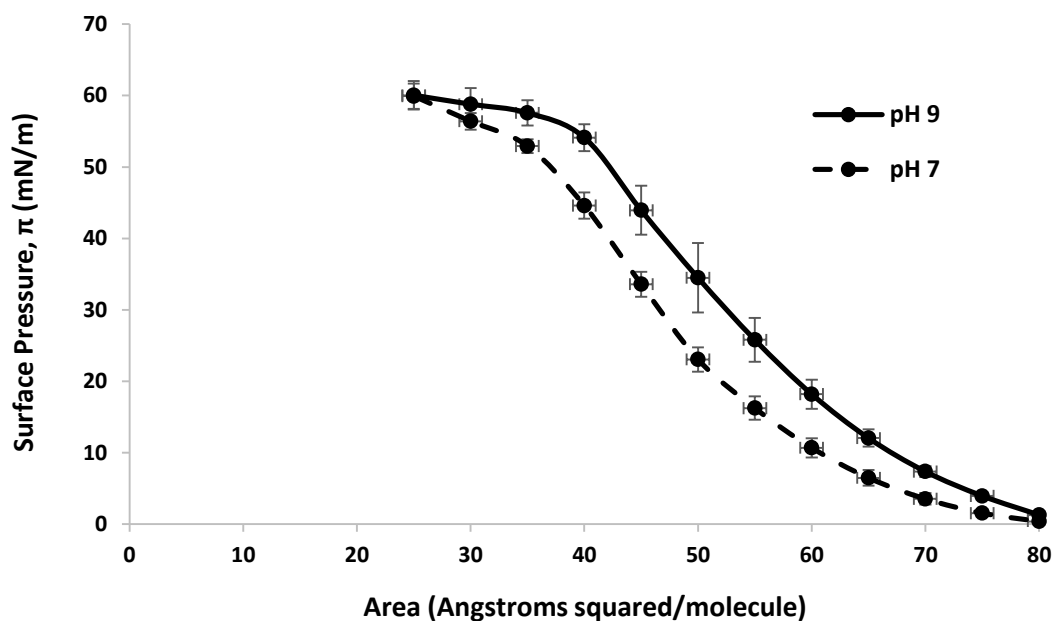


**Figure 3.** Langmuir  $\pi$ -A isotherms for the DPPC:POPG:PA system on a subphase of water at pH 7 and 9. The data are determined from a total of 3 repeats, with error bars displaying the standard error of the mean. Temperature:  $20 \pm 1^\circ\text{C}$ .

In both cases, it is evident that as the mixed monolayer is compressed there is a rise in surface pressure producing a smooth curve with gradient changes indicative of phase transitions within the surfactant film [42]. The mixed system at both pH values reaches an identical maximum surface pressure of 60mN/m. Furthermore, the lift-off area is similar between each system, and instantaneous at  $80\text{Å}^2/\text{molecule}$ . However, differences do arise when consideration is given to parameters such as the AUC, which is the largest for pH 9 (i.e. 100% at pH 9 and 86% at pH 7). The data signify that the molecules are in a more expanded state at pH 9. This observation is corroborated by the limiting area-per-molecule ( $A_{\text{lim}}$ ) values of  $72\text{Å}^2/\text{molecule}$  for pH 9 and  $59\text{Å}^2/\text{molecule}$  for pH 7.

## 3.2 Nicotine Administration

### 3.2.1 Nicotine – Simulated Pulmonary Surfactant Monolayer Interaction at pH 7

Langmuir pressure-area isotherms of the mixed surfactant systems were acquired at pH 7 in the absence and presence of nicotine, the results obtained are illustrated in Figure 4.

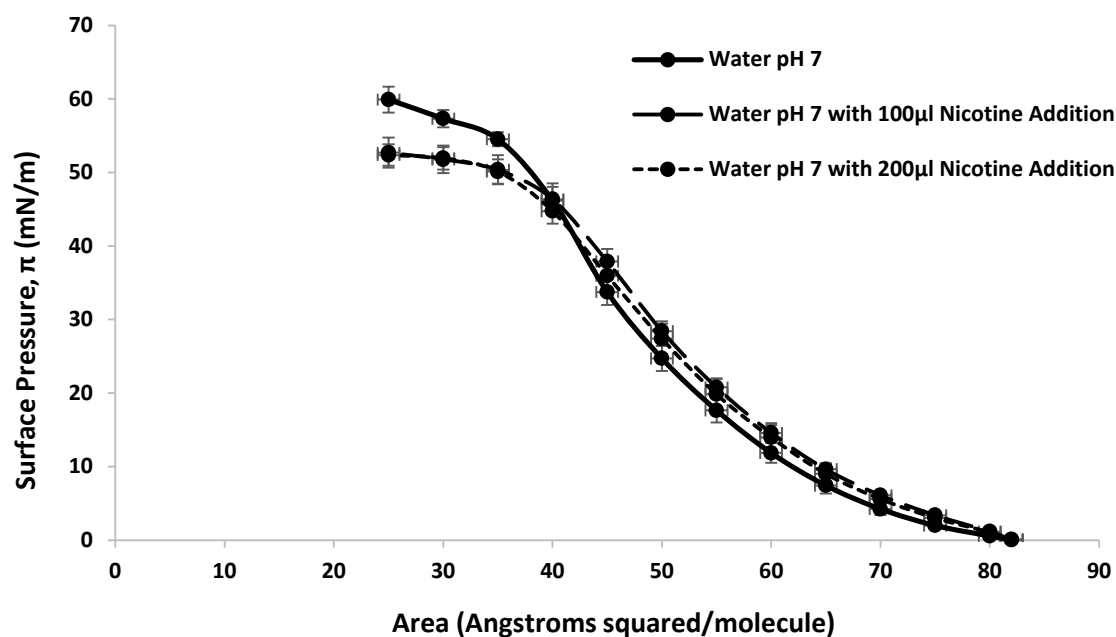


**Figure 4.** Average compression isotherms ( $n=3$ ) for the simulated monolayer system supported on a pH 7 subphase before and after nicotine addition. Temperature:  $20\pm 1^\circ\text{C}$ .

The addition of 100μl and 200μl of nicotine to the underside of the mixed surfactant monolayer lowered the maximum surface pressure from 60mN/m to 52mN/m. In addition, the AUC decreased from 100% to 97.4% (100μl nicotine) and 95.4% (200μl nicotine). On inspection of the data presented in Figure 4, the Langmuir isotherm acquired on the nicotine-containing subphases demonstrate a deviation to the right at low surface pressures, implying that the monolayer exhibits an expanded character. This point is further supported by  $A_{lim}$  values, which increase from  $60\text{Å}^2/\text{molecule}$  (pH 7), to  $67\text{Å}^2/\text{molecule}$  (100μl and 200μl nicotine). Compressibility values of 0.0122mN/m were observed following addition of both volumes of nicotine, in comparison to a baseline value of 0.0115mN/m, which equates to a 6% increase in the parameter. The data confirm that there is no significant difference in effect when 100μl or 200μl of nicotine are delivered to the underside of the mixed surfactant monolayer at pH 7. This confirms that in the case of the lower concentration of nicotine, the surfactant film is saturated with the molecules in solution.

### 3.2.2 Nicotine – Simulated Pulmonary Surfactant Monolayer Interaction at pH 9

Langmuir pressure-area isotherms of the mixed surfactant systems were acquired at pH 9 in the presence and absence of nicotine, the results obtained are detailed in Figure 5.

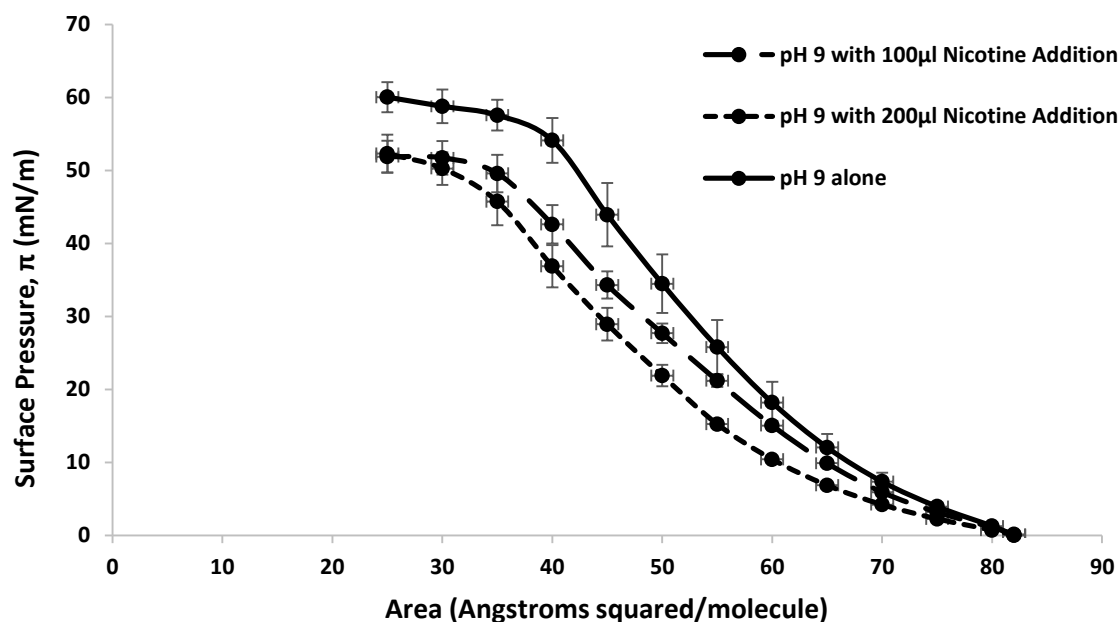


**Figure 5.** Average compression isotherms ( $n=3$ ) for the simulated monolayer system supported on a pH 9 subphase before and after nicotine addition. Temperature:  $20\pm 1^{\circ}\text{C}$ .

The delivery of nicotine to the aqueous subphase induces clear changes to the Langmuir isotherms at pH 9. There is a clear reduction in maximum surface pressure, from 60mN/m (pH 9 alone) to 52mN/m following the addition of 100μl or 200μl of nicotine solution. In this case, there is a strong dose-response translocation of the curves to the left side. The AUC reduces substantially more at pH 9 than at pH 7 on nicotine addiction and in a clear dose-response fashion from 100% to 83% and 76%. This trend is also confirmed via the compressibility values, rising from 0.0105mN/m (pH 9 alone) to 0.0127mN/M and 0.0130mN/M (pH 9 with 100μl and 200μl addition, respectively); equating to a 24% increase. As such, the film becomes less rigid and more compressible. The  $A_{lim}$  term corroborates this finding as it decreases from 72Å<sup>2</sup>/molecule to 64Å<sup>2</sup>/molecule (100μl nicotine) and 61Å<sup>2</sup>/molecule (200μl nicotine), clearly moving towards lower area per molecule.

On delivery of nicotine to the underside of the simulated pulmonary surfactant film, deviation in surfactant activity was evident irrespective of solution pH. The ionisation state of the nicotine molecule is an important factor to consider when attempting to rationalise the study findings. This is so because the charge distribution within the nicotine molecule will govern how the entity will interact with the neighbouring surfactant film.

Following protonation, the nitrogen atom in the pyrrolidine ring becomes positively charged [43]. Whilst the components of the model surfactant film applied herein are at a constant charge between pH 6 to 11. Within this pH range, the DPPC molecule exists as a zwitterion and the POPG and PA molecules demonstrate overall anionic character [43]. Accordingly, the molecular potential of each component within the systems of interest can be applied to explain key mechanisms of interaction. On addition of nicotine to an ultrapure water subphase at pH 7, the simulated pulmonary surfactant monolayer demonstrates expanded character. Here, the protonated nitrogen atoms within the nicotine structure (i.e. located on the pyrrolidine ring) bind to the negatively charged moieties within the monolayer structure via electrostatic interactions. The nature of interaction facilitates the ready insertion of the nicotine molecule into the two-dimensional ensemble and as such the spatial arrangement is modified, leading to a change in molecular packing along the two-dimensional plane. The net effect is a weakening of the intermolecular forces (e.g. van der Waals interactions) between each molecule forming the monolayer. Such interactions cause disruption and expansion to the monolayer [44], which consequently increases the pressure required to compress the ensemble (i.e. an elevation in compressibility was noted of 6%).

In the case of pH 9, the Langmuir isotherm and isocycles experience a translocation to the left side. This clear trend confirms condensed character, meaning that each molecule within the ensemble occupies a smaller area within that available on the surface. As nicotine is basic in nature, it is to be expected that at alkaline pH the molecule will exist predominantly in the neutral form. At pH 9, there is a greater proportion of non-protonated nicotine as compared to protonated nicotine within the aqueous environment [43]. The region of negative potential in the neutral form can interact with the positively charged end of the DPPC molecules and provide shielding of this positive charge which would reduce electrostatic repulsion with adjacent DPPC molecules. Hence, there is scope for the nicotine molecules to bind, in the main, with the DPPC molecules and consequently condense the monolayer [44].



### 3.2.3 Langmuir Isotherms at pH 7 and pH 9 with and without Nicotine Addition

Average Langmuir compression-expansion cycles of the mixed surfactant film located on an ultrapure water subphase at pH 7 before and after addition of 100  $\mu$ l nicotine solution are presented in Figure 6. The data presented are averages of eight consecutive compression-expansion cycles, to allow for confidence in the differences observed.

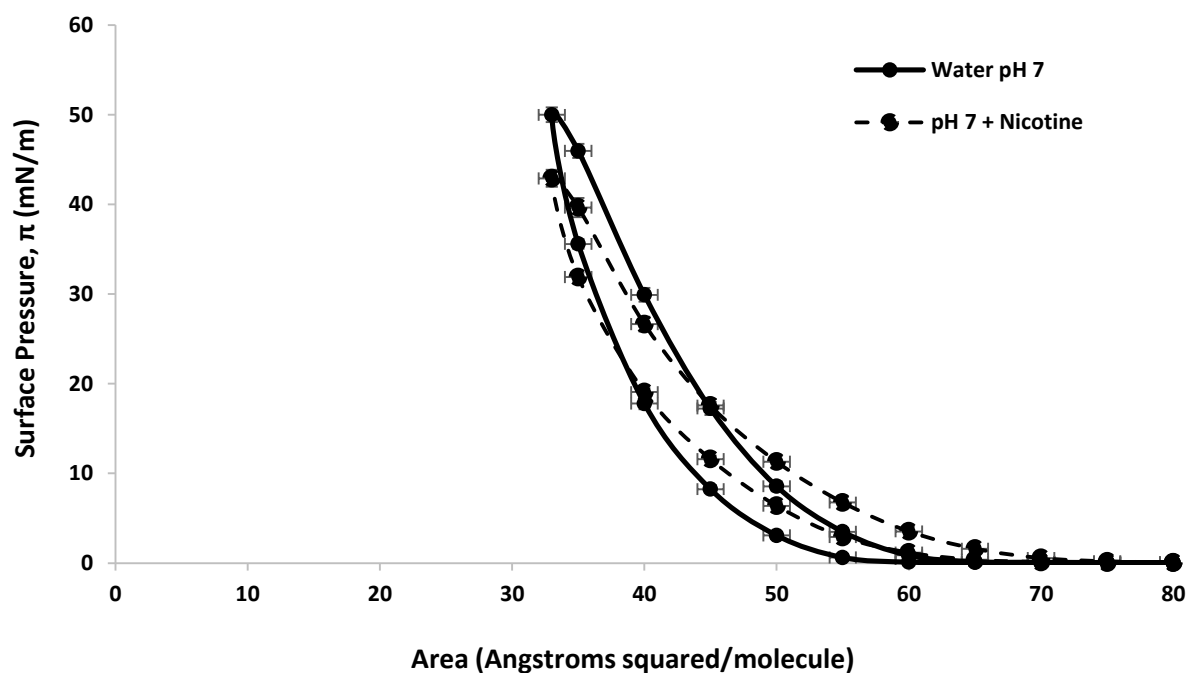


**Figure 6.** Averaged  $\pi$ -A compression-expansion cyclic isotherms ( $n=3$ ) for the mixed surfactant system on an ultrapure water subphase at pH 7, before and after 100 $\mu$ l nicotine administration. Temperature:  $20\pm 1^\circ\text{C}$ .

Upon inspection, a reduction in maximum surface pressure for the mixed surfactant monolayer when located on a nicotine containing subphase is apparent (e.g. a decline from 50mN/m to 42mN/m on surfactant films initially pre-conditioned to the equilibrium point via 4 compression-relaxation cycles). The data are consistent with that presented in Figure 4. In addition, the lift-off area value was greater when nicotine was applied to the underside of the surfactant film, being approximately 70  $\text{\AA}^2/\text{molecule}$  as compared to 62 $\text{\AA}^2/\text{molecule}$  with the pure-water subphase. Moreover, the AUC reduced from 100% to 95.9% on nicotine addition plus the compressibility of the film increased from 0.00902mN/m to 0.0110mN/m (i.e. a 23% increase, demonstrating reduced rigidity and enhanced flexibility). The hysteresis area of the isotherms (i.e. the area between compression and expansion) decreased on nicotine administration by 29mN/m.

Average Langmuir compression-expansion cycles of the mixed surfactant film located on an ultrapure water subphase at pH 9 before and after addition of 100 $\mu$ l nicotine solution are presented in Figure 7. Again, the data are averages of eight consecutive compression-expansion cycles after a period of material pre-conditioning to the equilibrium point (e.g. a total of four compression-relaxation cycles at the beginning of the experiment).

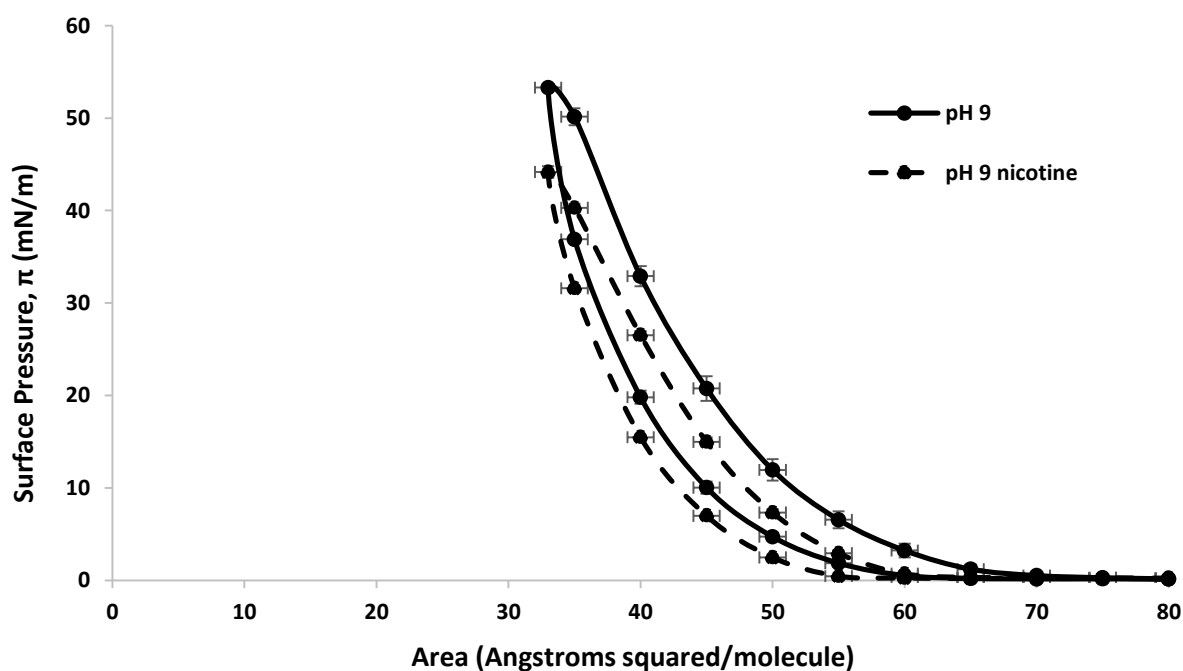


**Figure 7.** Averaged Langmuir  $\pi$ -A compression-expansion cyclic isotherms ( $n=3$ ) for the mixed surfactant system on an ultrapure water subphase at pH 9, before and after 100 $\mu$ l nicotine administration. Temperature:  $20 \pm 1^\circ\text{C}$ .

The data confirm that upon nicotine addition to the underside of the mixed surfactant film at pH 9, clear interaction between each species takes place. There is a notable reduction in maximum surface pressure from 53 mN/m to 44 mN/m along with movement of the curve to the left side. In addition, the lift-off area reduces from 68  $\text{Å}^2/\text{molecule}$  to 60  $\text{Å}^2/\text{molecule}$ , again the data set reflects that presented in Figure 5. Further to this, there is a significant reduction in the AUC term from 100% to 78.6% and an increase in the compressibility value by 24%, suggesting enhanced flexibility across the plane. Moreover, the hysteresis area of the isotherms presented shows a significant difference from pH 7, with a value of reduction of 80mN/m.

When considering the dynamic compression – expansion cycles at pH 7 and pH 9, the addition of nicotine to each system results in similar trends to single Langmuir isotherms. In the case of pH 7, there is an initial monolayer expansion and a decrease in the maximum surface pressure attained. Whereas, at pH 9 the system demonstrates initial condensation with a reduced maximum surface pressure. In both cases, the simulated pulmonary surfactant monolayer is capable of fulfilling its primary function of reducing the surface tension term (i.e. structure-function activity is not lost), which is clearly important for efficient lung mechanics. Notwithstanding this point, the presented data do confirm that the systems would have become more condensed over time with the POPG molecule being effectively ‘squeezed out’ of the two-dimensional plane [2]. In this case, the surfactant film would exhibit increased rigidity due to loss / reduction of the key fluidiser molecule. A similar trend was documented by Bringezu and co-workers in 2003, where a simulated pulmonary surfactant monolayer of the same composition became condensed and demonstrated lower maximum surface pressure on repeated expansion-compression cycles [1]. The effective ‘loss’ of the fluidiser into the surface associated reservoir highlights the requirement for regular replenishment of the components forming pulmonary surfactant otherwise the surface tension term would remain high and this would consequently increase the work of breathing.

### *3.3 Molecular Modelling*

#### *3.3.1 Nicotine Interaction with Surfactant Film Components at pH 7*

The electrostatic potential surfaces (EPSs) of the polar head groups associated with each surfactant molecule under investigation plus the whole nicotine molecule were calculated via the quantum mechanics software package Gaussian09, as previously described. Variable colour presentation symbolises differences in charge distribution across each functionality; where red indicates strongly negative regions, yellow less negative regions, blue strongly positive regions and cyan less positive regions. Regions coloured green have an approximately neutral electrostatic potential. In addition, we have inserted arrows to highlight important regions of interaction between the particular sections of the molecules under consideration.

The EPSs presented in Figure 8 represent nicotine in its pyrrolidine-protonated state alongside the polar head regions of DPPC and POPG. At pH 7, the nicotine molecule is predominantly (i.e. 60%) in this mono-protonated state [22 & 23]. The positively charged region within the nicotine molecule (i.e. blue region) will interact favourably with the negatively charged moieties within each of the amphiphilic molecules within the mixed surfactant film.

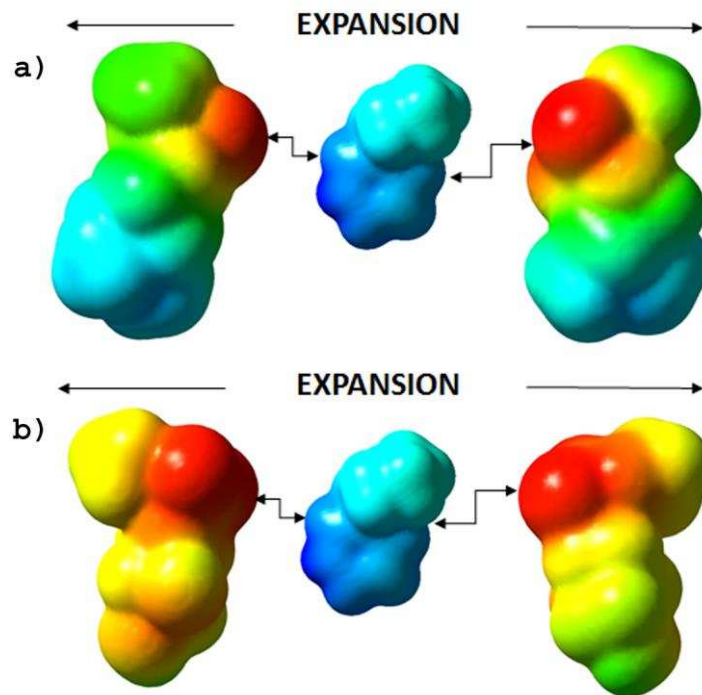


**Figure 8.** *EPS of calculation for the predominant phospholipid species within the mixed surfactant monolayer: a) DPPC and b) POPG. The head groups are displayed on the right and left side of the protonated nicotine molecule located in the middle present at pH 7. NB: Only the polar head groups are represented here. The hydrophobic tail functionalities (not included in the calculation) would extend up and away from the normal of the air-liquid interface.*

The DPPC and POPG molecules contain their negatively charged phosphate moieties within the head groups and thus are located further into the membrane (i.e. closer to the alveolar air-liquid interface). In this case, we suggest that the nicotine molecule must penetrate into the monolayer structure to permit interaction. Such penetration into the monolayer structure will most likely occur at low surface pressures whilst the monolayer is expanded in the gaseous phase.

The open positioning of the molecules will facilitate nicotine entry into the two-dimensional ensemble. Therefore, if the nicotine molecule is physically inserted between the head groups of DPPC and POPG the surfactant film should have a reduced ability to fully compress and the monolayer would exhibit an expanded character. Here, the interaction is predominantly based upon electrostatic associations. Indeed, this finding is consistent with the work conducted by Khattari and co-workers in 2011 [30]. This group applied a cationic surfactant to methyl octadecanoate (MO) monolayers and noted a deviation within the experimental data; larger molecular areas were found. The study established that the cationic surfactant became integrated into the monolayer structure. As anticipated, at higher surface pressures the monolayer is in a more condensed state. Here, the lipid fractions experience hydrophobic interactions between the acyl chains to a greater extent. At this point in the compression – expansion cycle, the interactions are indeed strong enough to prevent the further penetration of nicotine molecules. This principle has been demonstrated by Silva and Romao [45] along with Grancelli and co-workers [46] who detailed that such compaction does not permit molecular species within solution to insert themselves amongst amphiphilic head groups. Therefore, we propose that at high surface pressures, the neutral regions of DPPC and nicotine at pH 7 associate by hydrophobic interactions and force DPPC out of its usual plane, resulting in impairment of the surface tension lowering capability.

### *3.3.2 Nicotine Interaction with Surfactant Film Components at pH 9*

Within aqueous media at pH 9 the nicotine molecule is primarily (90%) in the neutral form [22]. Under such conditions, the lone pair on the nitrogen atom of the pyridine ring presents a compact region of negative potential. This charge distribution is presented as the red region in the EPS calculation, with the remainder of the molecule being neutral, as illustrated in Figure 9.

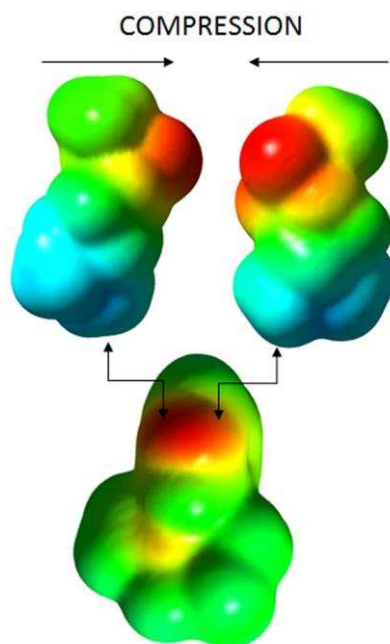


**Figure 9.** EPS of DPPC (right and left) and neutral nicotine (middle) at pH 9.

The *in-silico* data indicate that the pyridine ring within the nicotine molecule can interact with the positive charge held within the DPPC polar head group (i.e. the charged trimethylammonium group (blue)). Here, nicotine is able to interact with DPPC molecules without necessitating penetration of the monolayer during expansion, hence the interaction may persist during all stages of compression-expansion. These interactions explain the consistent shift to the left of the isotherms, signifying a transformation to lower area per molecule and the formation of a more condensed monolayer. The location of this grouping close to the air-liquid interface renders nicotine capable of interacting at the interfacial regions, without having to penetrate into the monolayer to any great depth. Consequently, a reconfiguration of the lipid arrangement occurs with the DPPC molecules held closer together.

### 3.3.3 Nicotine interaction with components of the surfactant to reduce the surface pressure

With reference to all Langmuir isotherm and isocycle data presented within this study, there is a clear reduction in the surfactant surface pressure term following nicotine administration to the supporting aqueous media. This trend may be rationalised by reference to the EPS calculation detailed in Figure 10.

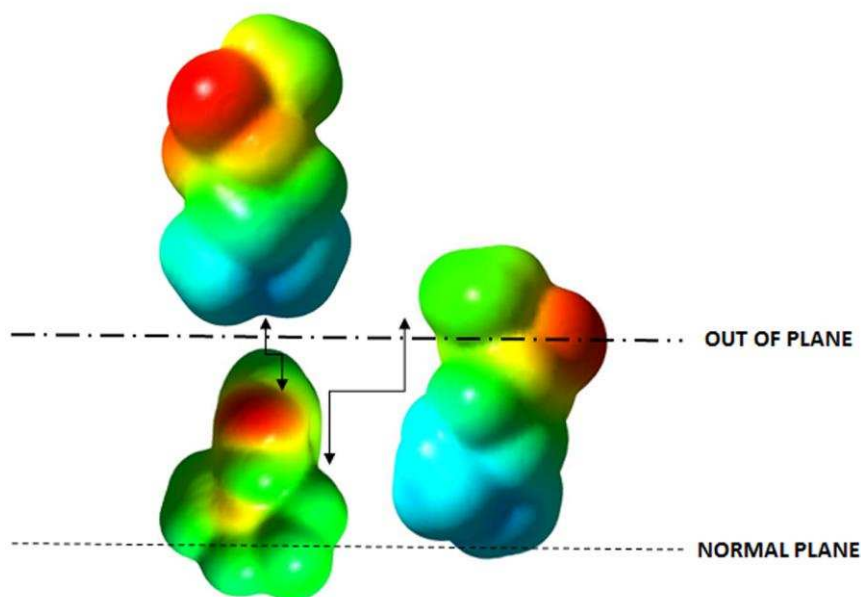


**Figure 10.** EPS calculation of the polar head groups of DPPC (right and left) and neutral nicotine (middle).

At pH 7, nicotine is approximately 40% in the neutral form and its surface is substantially neutral. Neutral regions are similarly noted in the DPPC molecules; specifically in the region of the two CH<sub>2</sub> groupings between the phosphate moiety and the charged trimethylammonium group. Consequently, these two uncharged zones can interact with each other via hydrophobic associations. As such, when nicotine is located between two phospholipid head groups it can undergo electrostatic interactions with the positive charge on one of the DPPC molecules and hydrophobic interactions with the other DPPC molecule. This interaction requires the DPPC molecules to slide out of alignment and would result in a shearing effect between the molecules. Ultimately, this can facilitate the buckle and collapse of the monolayer at higher surface pressures and hence a reduced maximum surface pressure term ( $\pi$ ). Furthermore, due to the DPPC molecules being outside of the normal plane the surfactant molecules have reduced contact with the aqueous media, which subsequently hinders the capacity to reduce the surface tension term.

Because the DPPC molecule presents as the largest lipid fraction within the model blend used in this study, it is reasonable to assume that the interaction between that component and nicotine is primarily responsible for the reduction in the maximum observed surface pressure. This point is strengthened if we consider DPPC as the main 'stabiliser' molecule within the ensemble [47]. Here, the main function is to keep the monolayer rigid enough to attain near-zero surface tensions during exhalation. Thus, if the bulk of the DPPC molecules are interacting with, and consequently being disrupted by nicotine molecules, scope to perform the stabilisation role is limited.

During this work we have considered each interaction individually. However, the array of interactions throughout the surfactant film will be the result of interaction of the nicotine molecules with a number of surrounding molecules, each of which we would expect to maximise its attractive interactions or else avoid coming into contact with the drug (i.e. by diffusing across the membrane) in cases where no attractive interactions are possible.

### *3.4 Public Health*

The use of cigarettes / e-cigarettes is a common practice within developed countries such as the United Kingdom and the United States of America. Despite the attempts made by various government and health agencies to educate the population and minimize exposure to tobacco smoke, thousands of individuals experience long-term respiratory diseases that impact upon health, wellbeing and quality of life. By demonstrating the undesirable effects of nicotine on the molecular level, extrapolation of laboratory and *in silico* data can be used to highlight potential negative implications to the human body.

The delivery of nicotine to the underside of simulated pulmonary surfactant caused a reduction in the surface pressure term in all cases. The data confirm that the ability of the surfactant film to reduce the surface tension was impaired, which would in turn result in an increased work of breathing. The situation may give rise to respiratory distress syndrome, which can affect neonates and adults. The disorder further results in impaired gas exchange, atelectasis (collapse or incomplete inflation of the lung), hypoxia, oedema, pulmonary hypertension and other associated complications [48 & 49]. Over time, such impairment to lung function can cause severe respiratory disorders including oedema and inflammation. Clearly, these conditions can further impair the surfactant system and lead to a reduction in the quality of life [1 & 50].



Moreover, the increase in surface compressibility in nicotine's presence corresponds to a smaller change in surface tension compared to surface area, and physiologically this translates to a decrease in the range of alveolar volumes over which surface tension contributes to alveolar stability [29]. Related disease presentation may include; respiratory distress syndrome, obstructive lung disease (COPD, asthma, bronchiolitis) and interstitial lung disease; all are linked by their comparable pathogenesis [49]. Interstitial lung diseases can be described as restrictive ventilator defects, which are related to restricted lung expansion, decreased lung volume and an increased work of breathing [51].

#### **4. Conclusion**

This study has clearly demonstrated that the addition of nicotine to an aqueous environment supporting a simulated pulmonary surfactant monolayer does cause modification to the activity profile of the amphiphilic material. All experiments were conducted in model conditions (i.e. ultrapure water instead of salts, no surfactant proteins and spread monolayer without subphase reservoirs of surfactant material), however clear trends in the data are apparent and enable appropriate rationalisation and extrapolation to the human respiratory system. Of the data collected, the pH 7 series is the most physiologically relevant as it reflects the value of the biological media within the lung. The data confirm that the addition of nicotine expands the monolayer and impairs the ability to reduce the surface tension term; modelling data have provided a mechanistic explanation for this.

This work provides a unique insight into how nicotine, the predominant molecule within cigarette vapour, can potentially influence lung function. The interaction between each species may contribute to a number of disease states and cause the individual to experience breathlessness after smoking along with an increased respiratory rate to provide the body with adequate oxygen levels. Longer term consequences can involve the presentation of COPD and interstitial lung diseases.

The combination of Langmuir monolayer technology with modelling techniques has provided a strong platform by which to better understand the interaction between the nicotine molecular and material presenting at the alveolar air-liquid interface. Expansion of this work could involve further investigation relating to how other components of cigarette / e-cigarette vapour may influence surfactant function, typical examples for consideration include formaldehyde and ammonia.

## 5. Acknowledgements

MJD would like to thank LJMU for supporting this research effort. Special thanks go to Mr Paul Burgess and Mr Geoffrey Henshaw for the support provided throughout.

## 6. References

1. F. Bringezu, K. Pinkerton, J. Zasadzinski, Environmental Tobacco Smoke Effects on the Primary Lipids of Lung Surfactant. *Langmuir* 19(7) (2003) 2900-2907.
2. J. Zasadzinski, J. Ding, H. Warriner, F. Bringezu, A. Waring, The physics and physiology of lung surfactants. *Current Opinion in Colloid & Interface Science*. 6(5-6) (2001) 506-513.
3. J. Scott, The Pulmonary Surfactant: Impact of Tobacco Smoke and Related Compounds on Surfactant and Lung Development. *Tob. Induced Dis.* 2(1) (2004) 1.
4. S. Duncan, R. Larson, Comparing Experimental and Simulated Pressure-Area Isotherms for DPPC. *Biophysical Journal*. 94(8) (2008) 2965-2986.
5. S. Yu, F. Possmayer, Interaction of pulmonary surfactant protein A with dipalmitoylphosphatidylcholine and cholesterol at the air/water interface. *Journal of Lipid Research*. 39(3) (1998) 555-568.
6. R.H. Notter, Lung Surfactants, Basic Science and Clinical Applications. *Lung Biology in Health and Disease*. New York, Marcel Dekker, 2000.
7. J. Miñones, J. Rodríguez Patino, O. Conde, C. Carrera, R. Seoane, The effect of polar groups on structural characteristics of phospholipid monolayers spread at the air–water interface. *Colloids and Surfaces A: Physicochemical and Engineering Aspects*. 203(1-3) (2002) 273-286.
8. M.J. Davies, T. Kerry, L. Seton, M.F. Murphy, P. Gibbons, J. Khoo, M. Naderi, The crystal engineering of salbutamol sulphate via simulated pulmonary surfactant monolayers. *International Journal of Pharmaceutics*. 446(1-2) (2013) 34-45.
9. B. Fleming, C. Raynor, K. Keough, Some characteristics of monolayers of 1-palmitoyl-2-oleoyl-phosphatidylglycerol with and without dipalmitoylphosphatidylcholine during dynamic compression and expansion. *Biochimica et Biophysica Acta (BBA) – Biomembranes*. 732(1) (1983) 243-250.
10. F. Bringezu, J. Ding, G. Brezesinski, J.A. Zasadzinski, Changes in Model Lung Surfactant Monolayers Induced by Palmitic Acid. *Langmuir*. 17 (2001) 4641-4648.

11. M.J. Davies, L. Seton, N. Tiernan, M.F. Murphy, P. Gibbons, Towards crystal engineering via simulated pulmonary surfactant monolayers to optimise inhaled drug delivery. *International Journal of Pharmaceutics*. 421 (2011) 1–11.
12. W. Zhao, T. Róg, A. Gurtovenko, I. Vattulainen, M. Karttunen, Atomic-Scale Structure and Electrostatics of Anionic Palmitoyloleoylphosphatidylglycerol Lipid Bilayers with Na<sup>+</sup> Counterions. *Biophysical Journal*. 92(4) (2007) 1114-1124.
13. R. Veldhuizen, K. Nag, S. Orgeig, F. Possmayer, The Role of Lipids in Pulmonary Surfactant. *Biochimica et Biophysica Acta*. 1408 (1998) 90-108.
14. J. Ding, I. Doudevski, H.E. Warriner, T. Alig, J.A. Zasadzinski, Nanostructure Changes in Lung Surfactant Monolayers Induced by Interactions between Palmitoyloleoylphosphatidylglycerol and Surfactant Protein B. *Langmuir*. 19 (2003) 1539-1550.
15. J. DeRuiter, Carboxylic Acid Structure and Chemistry: Part 1. *Principles of Drug Action*. 1 (2005) 1-3.
16. M.J. Davies, A. Brindley, X. Chen, S.W. Doughty, M. Marlow, C.J. Roberts, A quantitative assessment of inhaled drug particle–pulmonary surfactant interaction by atomic force microscopy. *Colloids and Surfaces B: Biointerfaces*. 73 (2009) 97-102.
17. C.P. Stenger, C. Alonso, J.A. Zasadzinski, J.A. Waring, C. Jung, E.K. Pinkerton, Environmental Tobacco Smoke Effects on Lung Surfactant Film Organization. *Biochimica et Biophysica Acta*. 1788(2) (2009) 358-370.
18. P. Jha, C. Ramasundarahettige, V. Landsman, B. Rostron, M. Thun, R.N. Anderson, T. McAfee, R. Peto, 21<sup>st</sup> Century Hazards of Smoking and Benefits of Cessation in the United States. *New England Journal of Medicine*. 368(4) (2013) 341-350.
19. WebMD. Lung Diseases - Overview. 2015. Accessed April 2016.
20. D. Elmore, D.A. Dougherty, Computational Study of Nicotine Conformations in the Gas Phase and in Water. *The Journal of Organic Chemistry*. 65(3) (2000) 742-747.
21. D. Burgermeister, Understanding Nicotine and Depression. *Journal for Nurse Practitioners*. 5(7) (2015) 1136-1149.
22. K. Pi, M. Xia, P. Wu, M. Yang, S. Chen, D. Liu, A. Gerson, Effect of Oxidative Modification of Activated Carbon for the Adsorption Behaviour of Nicotine. *J. Ind. Eng. Chem.* 31 (2015) 112-117.
23. J. Graton, M. Berthelot, J. Gal, S. Girard, C. Laurence, J. Labreton, P. Naus, Site of Protonation of Nicotine and Nornicotine in the Gas Phase: Pyridine or Pyrrolidine Nitrogen? *J. Am. Chem. Soc.* 124(35) (2002) 10552-10562.

24. J. Graton, T. Mourik, S. Price, Interference between the Hydrogen Bonds to the Two Rings of Nicotine. *J. Am. Chem. Soc.* 125(19) (2003) 5988-5997.
25. T. Clark, M. Hennemann, J.S. Murray, P. Politzer, Halogen bonding: the  $\sigma$ -hole. *Journal of Molecular Modelling.* 13 (2007) 291-296.
26. M. Mascal, A. Armstrong, M.D. Bartberger, Anion-aromatic bonding: a case for anion recognition by  $\pi$ -acidic rings. *J. Am. Chem. Soc.* 124 (2002) 6274-6276.
27. A.C. Hunter, Quantifying Intermolecular Interactions: Guidelines for the Molecular Recognition Toolbox. *Angew. Chem. Int. Ed.* 43 (2004) 5310-5324.
28. A.R. Shah, R. Banerjee, Effect of D- $\alpha$ -tocopheryl polyethylene glycol 1000 succinate (TPGS) on surfactant monolayers. *Colloids and Surfaces B.* 85 (2011) 116-124.
29. S. Subramaniam, P. Bummer, C.G. Gairola, Biochemical and Biophysical Characterization of Pulmonary Surfactant in Rats Exposed Chronically to Cigarette Smoke. *Fundamental and Applied Toxicology.* 27 (1995) 63-69.
30. Z. Khattari, U. Langer, S. Aliaskarsohi, A. Ray, M. Fischer, Effects of soluble surfactants on the Langmuir monolayers compressibility: A comparative study using interfacial isotherms and fluorescence microscopy. *Materials Science and Engineering C.* 31(8) (2011) 1711-1715.
31. F. Behroozi, Theory of Elasticity in Two Dimensions and Its Application to Langmuir–Blodgett Films. *Langmuir.* 12(9) (1996) 2289–2291.
32. A. Lucero, M.R. Rodriguez, A.P. Gunning, V.J. Morris, P.J. Wilde, J.M. Rodriguez, Effect of Hydrocarbon Chain and pH on Structural and Topographical Characteristics of Phospholipid Monolayers. *J Phys Chem B.* 112(25) (2008) 7651-7661.
33. P.J. Quinn, M. Kates, J.F. Tocanne, M. Tomoaia-Cotisel, Surface characteristics of phosphatidylglycerol phosphate from the extreme halophile *Halobacterium cutirubrum* compared with those of its deoxy analogue, at the air/water interface. *Biochem J.* 261(2) (1989) 377-381.
34. D. Attwood, T.A. Florence, *Physical Pharmacy: FastTrack 2<sup>nd</sup> Ed.*, Pharmaceutical Press, 2012.
35. C.C.J. Roothaan, New developments in molecular orbital theory. *Reviews of Modern Physics.* 23 (1951) 69.
36. G.G. Hall, In the molecular orbital theory of chemical valency. VIII. A method of calculating ionization potentials. *Proceedings of the Royal Society of London A: Mathematical, Physical and Engineering Sciences; The Royal Society.* 205 (1951) 541-552.
37. P.C. Hariharan, J.A. Pople, Influence of polarization functions on MO hydrogenation energies. *Theor. Chim. Acta.* 28 (1973) 213-222.
38. Gaussian 09, Revision C.01. M.J. Frisch, G.W. Trucks, H.B. Schlegel, G.E. Scuseria, M.A. Robb, J.R. Cheeseman, G. Scalmani, V. Barone, B. Mennucci, G.A. Petersson, H. Nakatsuji, M.

- Caricato, X. Li, H.P. Hratchian, A.F. Izmaylov, J. Bloino, G. Zheng, J.L. Sonnenberg, M. Hada, M. Ehara, K. Toyota, R. Fukuda, J. Hasegawa, M. Ishida, T. Nakajima, Y. Honda, O. Kitao, H. Nakai, T. Vreven, J.A. Montgomery, J.E. Peralta, F. Ogliaro, M. Bearpark, J.J. Heyd, E. Brothers, K.N. Kudin, V.N. Staroverov, R. Kobayashi, J. Normand, K. Raghavachari, A. Rendell, J.C. Burant, S.S. Iyengar, J. Tomasi, M. Cossi, N. Rega, J.M. Millam, M. Klene, J.E. Knox, J.B. Cross, V. Bakken, C. Adamo, J. Jaramillo, R. Gomperts, R.E. Stratmann, O. Yazyev, A.J. Austin, R. Cammi, C. Pomelli, J.W. Ochterski, R.L. Martin, K. Morokuma, V.G. Zakrzewski, G.A. Voth, P. Salvador, J.J. Dannenberg, S. Dapprich, A.D. Daniels, Ö. Farkas, J.B. Foresman, J.V. Ortiz, J. Cioslowski, D.J. Fox. Gaussian, Inc., Wallingford CT, 2009.
39. Omega, Version 2.5.1.4, OpenEye Scientific Software, Inc., Santa Fe, NM, USA, [www.eyesopen.com](http://www.eyesopen.com), 2010.
40. GaussView, Version 5, Dennington, Roy; Keith, Todd; Millam, John. Semichem Inc., Shawnee Mission, KS, 2009.
41. T. Wiedmann, A. Salmon, V. Wong, Phase Behavior of Mixtures of DPPC and POPG. *Biochimica et Biophysica Acta - Lipids and Lipid Metabolism*. 1167(2) (1993) 114-120.
42. V. Matti, J. Saily, S.J. Ryhanen, J.M. Holopainen, S. Borocci, G. Mancini, P.K. Kinnunen, Characterization of Mixed Monolayers of Phosphatidylcholine and a Dicationic Gemini Surfactant SS-1 with a Langmuir Balance: Effects of DNA. *Biophys J*. 81(4) (2001) 2135-2143.
43. Chemicalize.Org. [Chemicalize.org](http://Chemicalize.org). N.P. Accessed April 2016.
44. K. Kanisto, H. Yhteiskoulu, Effects of Nicotine on a Primary Lipid of Lung Surfactant: Testing the Stability and Efficiency Using Subphases of Different Ion Strengths and pH. 2006.
45. A. Silva, R. Romao, Mixed monolayers involving DPPC, DODAB and oleic acid and their interaction with nicotinic acid at the air–water interface. *Chemistry of Physics and Lipids*. 137 (2005) 62-76.
46. A. Grancelli, A. Morros, E.M. Cabanas, O. Domenech, S. Merino, J.L. Vasquez, M.T. Montero, M. Vinas, J. Hernandez-Borrell, Interaction of 6-Fluoroquinolones with Dipalmitoylphosphatidylcholine Monolayers and Liposomes. *Langmuir*. 18(24) (2002) 9177-9182.
47. Y.D. Takamoto, M.M. Lipp, A. Nahmen, K.Y. Lee, A.J. Waring, J.A. Zasadzinski, Interaction of Lung Surfactant Proteins with Anionic Phospholipid. *Biophys. J*. 81 (2001) 153-169.
48. H.R. Notter, Z. Wang, P.R. Chess, D.F. Willson, Pulmonary Surfactant: Biology and Therapy. *The Respiratory Tract in Paediatric Critical Illness and Injury*. Springer-Verlag. (2009) 109-110.
49. A. Akella, B.S. Deshpande, Pulmonary Surfactants and their Role in Pathophysiology of Lung Disorders. *Indian Journal of Experimental Biology*. 51 (2013) 5-22.

50. E. Putman, L.M. van-Golde, H.P. Haagsman, Toxic Oxidant Species and Their Impact on the Pulmonary Surfactant System. *Lung*. 175(2) (1997) 75-103.
51. J.H. Ryu, T.V. Colby, T.E. Hartman, R. Vassalla, Smoking-related Interstitial Lung Diseases: A Concise Review. *European Respiratory Journal*. 17 (2001) 122-132.